

## Chapter 4

# Design of High Quality Factor Photonic Crystal Nanocavities by Optimizing Slab Thickness

### 4.1 Introduction

As mentioned in chapter 2, complete control of light in three dimensions can be achieved in three-dimensional photonic crystal, which possesses a three-dimensional band gap. However, fabricating such an ideal structure has still been a great challenge due to the requirement of highly-advanced structural designs as well as fabrication techniques. Therefore, photonic crystal slab structure, which requires only relatively easy top-down fabrication process, is preferable. In order to minimize out-of-plane scattering loss what is called air-bridge photonic crystal slab structure, which is the photonic perforating dielectric slab cladded with air, is one of the most promising structures. However, in air-bridge slab structure, there are only gaps for guided modes not for all modes. Therefore radiation losses, which correspond to the mode locating above the light line, in the vertical direction still exist. When a defect is introduced to the slab to form a nanocavity, the vertical radiation loss will limit the  $Q$ -factor in the vertical direction. While the in-plane  $Q$ -factor can be increased exponentially with the number of photonic crystal layers surrounding the defect region, the vertical  $Q$ -factor will restrict the total  $Q$ -factor to only low values [25]. This is one of the most important obstacles for photonic crystal slab nanocavities to achieve high-efficiency light sources such as low threshold lasers and single-photon emitters. Many research groups have been paying their attentions to design the structures, which can reduce the vertical radiation losses. Thanks to the flexibility in the design of two-dimensional photonic crystal slab nanocavity, various designs of ultra-high  $Q$ -factor nanocavity have already been succeeded [8]-[13], [26]. However, most of designs of those structures are based on the modification of the defect structures, in which the high  $Q$  modes are very sensitive to their surrounding structural parameters, that is, these designs require a precise control of position and size of air holes in practical fabrication, in which the  $Q$ -factor significantly degrades when the structural parameters are deviated from their ideal setups [27]. This lack of robustness to

changes in the cavity geometry becomes a great difficulty to practically fabricate the device with quality as good as the simulation results.

In this chapter, a new approach to design high  $Q$ -factor photonic crystal nanocavities by just simply changing slab thickness without modification of structural parameters of air holes surrounding the defect cavities will be presented. The mode volume of the defect mode exploited in this design will be shown to be very small, smaller than a half cubic wavelength. Therefore, a very large Purcell factor is expected. In the next section, the structural parameters of the designed cavity will be described in details.

## 4.2 Structural Parameters and Defect Mode of the Design Cavity

In this section, details of structural parameters exploited in the FDTD calculation and defect mode of interest will be presented. The computational model of the design of the cavity is based on air-bridge type photonic crystal slab, which is the

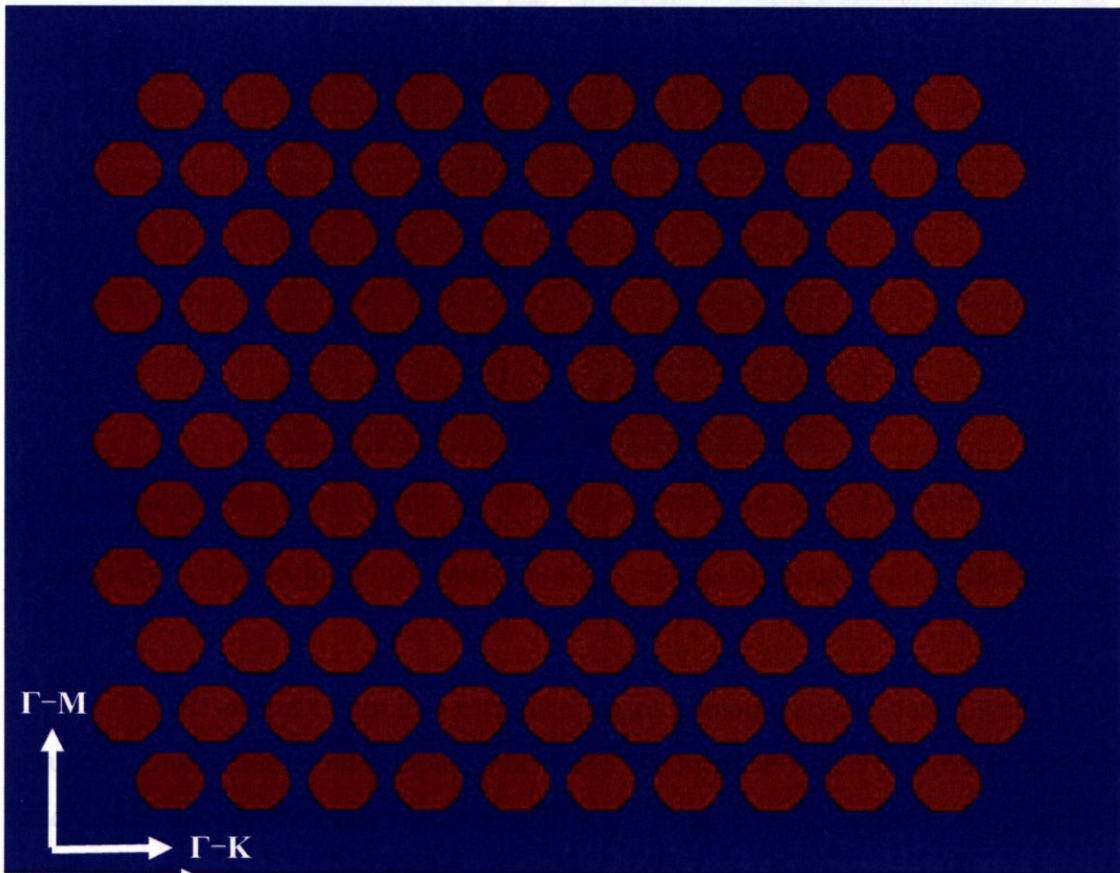


**Figure 4.1** Top-view of the H1-defect nanocavity in a 2D photonic crystal. Dark circles represent to air holes with refractive index of 1 etched into a slab with refractive index of 3.4.

dielectric slab with refractive index of 3.4 cladded with air, with a triangular lattice of air holes with lattice constant  $a$ . The top-view of the FDTD calculation model is shown in Fig. 4.1. The calculation domain contains eleven air holes along the  $\Gamma - K$  direction. The thickness of the slab and the radii of air holes are varied to various values to observe the dependence of cavity characteristics on these parameters, as will be described later. A defect is formed by simply removing one of air holes at the center as shown as a missing hole at the center in Fig. 4.1 and is called H1-defect structure.

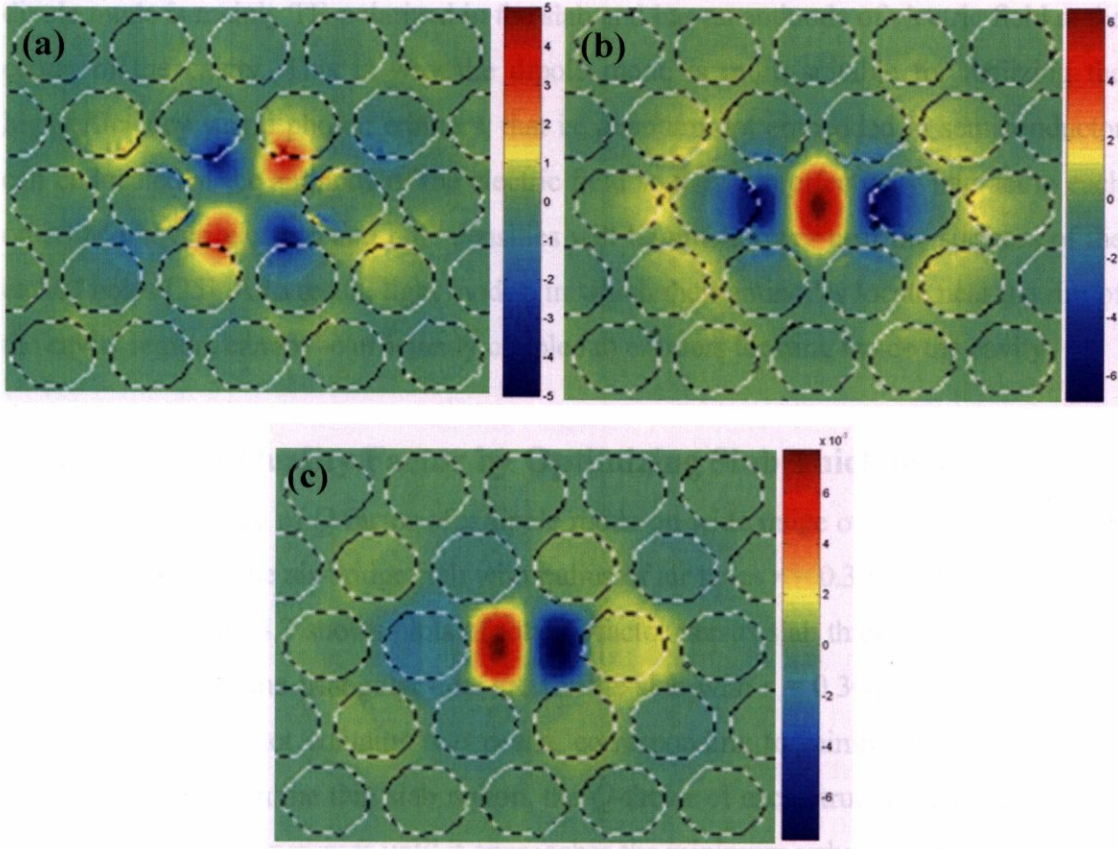


**Figure 4.2** Field distributions of the dipole mode of the H1-defect structure detected at the center of the slab (a)  $E_x$  component, (b)  $E_y$  component, and (c)  $H_z$  component. The circular dotted lines show the regions of air holes for reference.

The H1-defect cavity in a triangular lattice photonic crystal slab is well-known to support doubly-degenerated dipole modes in a band gap, in which  $Q$ -factor is only few hundreds in the conventional structure with parameters  $d = 0.50a$  and  $r = 0.30a$  [28]. Figure 4.2 shows top-view of field distributions of  $E_x$ ,  $E_y$ , and  $H_z$  components of  $x$  dipole mode, which has been concentrated in this chapter, at the center of the slab. Only these three components are illustrated because the structure is designed to support the TE-like

modes. Some attempts to increase the  $Q$ -factor of the dipole mode have been reported, such as changing the refractive index of the defect region [25] or modifying shape, size, and position of the nearest neighbor air holes surrounding the defect region [12]. However, it is pretty difficult to apply those high- $Q$  modes to practical devices. There have also been other trials to find additional defect modes, which have much higher  $Q$ -factor than dipole mode, such as monopole and hexapole mode, in H1-defect structure by reducing and pushing away the nearest neighbor air holes [4], [13], [29]. But these modes have a node of electric field in the high-index region at the cavity center, while the dipole mode is mainly TE-polarized in the slab and has an antinode of electric field at the center of the cavity. This is why the dipole mode is more suitable for realizing the high-efficiency single photon emitters, that is, quantum dot embedded in semiconductor can be located at the antinode of the electric field so they can effectively interact to each other. Moreover, electron and hole densities will be much lower near the surfaces of the etched holes [25]. As a result, light modes, in which their antinodes locate near the rim of the cavity region, cannot be efficiently coupled to emitters locating inside the cavity

### 4.3 Increase of Quality Factor by Optimizing Slab Thickness

Dependence of  $Q$ -factor of  $x$  dipole mode on wide range of slab thickness, from  $0.65a$  to  $1.75a$ , for the air-bridge slab with radius of air holes  $r = 0.30a$ ,  $0.35a$ , and  $0.40a$ , was studied. Figure 4.3 shows plots of total  $Q$ -factor versus slab thickness, where boxed dots, circular dots, and triangular dots are for the slab with  $r = 0.30a$ ,  $0.35a$ , and  $0.40a$ , respectively. Each plot contains two peaks, corresponding to minimum and maximum values of  $Q$ -factor. In the thin slab region, the  $Q$ -factor of each structure gradually drops as the slab thickness increases until it approaches the minimum value. After the minimum point, while the slab thickness keeps increasing, the  $Q$ -factor abruptly enhances to the maximum value and then decreases again. The highest  $Q$ -factor reaches the value of 16,200 when the radius of air holes and the slab thickness are equal to  $0.40a$  and  $1.35a$ , respectively. The highest  $Q$ -factor for the structures with  $r = 0.30a$  and  $0.35a$  are about 1,100 and 3,500, respectively. In addition, the peak of the  $Q$ -factor of the structure with  $r = 0.40a$  occurs at the thinnest slab followed by that of the structure with  $r = 0.35a$  at the slab thickness of about  $1.45a$ . The peak of the  $Q$ -factor of the structure with  $r = 0.30a$  is obtained at the thickest slab of about  $1.55a$ .